Computation of Steady and Unsteady Control Surface Loads in Transonic Flow

Bala K. Bharadvaj*
Douglas Aircraft Company, Long Beach, California 90846

A computational procedure for the analysis of loads due to steady and oscillatory control surface deflections is presented. The numerical algorithm is based on a time accurate solution of the transonic full potential equation in a body-fitted coordinate system. Control surface deflection and motion are modeled using an equivalent body velocity that circumvents the need for generating time-dependent grids and interpolation between planes and discontinuity. Viscous effects, including mild separation, are modeled using an interactive inverse boundary layer and the transpiration velocity approach. Numerical results are presented for a three-dimensional transport aircraft wing with supercritical sections, for control surfaces located at the trailing edge and the leading edge, for steady as well as oscillatory deflections. Results are compared with experimental data as well as with linear theory.

Introduction

THE accurate prediction of unsteady control surface loads is becoming increasingly important because of recent developments in the technology for flutter suppression, load alleviation, and improving aircraft performance and stability. Inviscid analysis procedures based on transonic small disturbance theory[1] and full-potential theory[2] have been reported previously. However, it is widely recognized that viscous effects, including shock/boundary-layer interaction play a significant part in transonic flow. Therefore, it is necessary to develop efficient analysis methods, including the effects of viscosity, to simulate the aerodynamics of control surfaces in transonic flow.

In principle, this problem can be addressed by computational methods based on the Navier-Stokes equations. However, at the present time, Navier-Stokes techniques typically require large amounts of computational time and expert users. Therefore, inviscid methods that account for viscous effects through interactive boundary-layer analysis provide a more efficient alternative for many practical problems. For two-dimensional problems, it has been shown that inviscid flow analysis with an interactive boundary layer can yield results comparable in accuracy to those obtained from thin-layer Navier-Stokes analysis.[3] This technique has also been used to analyze two-dimensional flows with separation.[4] Solution procedures based on inviscid/viscous analyses have been applied to steady flow past three-dimensional wings demonstrating a substantial improvement in the accuracy of the results (e.g., see Refs. 5 and 6). This approach has been used to study unsteady flows in two dimensions using various inviscid formulations (e.g., see Refs. 7–9). However, applications to unsteady three-dimensional flows are comparatively limited;[10] the author is not aware of any previous applications to the analysis of three-dimensional wings with control surfaces.

Formulation

The potential flow formulation used in the present time-accurate analysis is based on the strongly implicit approximate factorization scheme due to Stone[11] as implemented previously by Malone and Sankar.[12] A body-fitted sheared parabolic C-H grid is used. The time accuracy is improved by using Newton iterations at each time step.

For three-dimensional wings without control surfaces, the standard potential flow boundary conditions are used, i.e., freestream conditions far away from the body, nonpenetration at the body surface, and potential jump across the wake.

Control Surface Modeling

Using the standard boundary conditions for analyzing wings with unsteady control surface deflection introduces two new issues that need addressing. When a control surface is deflected, it modifies the section geometry of the original wing. For two-dimensional steady flow problems, this can be accounted for by modifying the grid and applying the standard boundary conditions as done in Ref. 13. However, when the control surface deflection is unsteady, the section geometry becomes a function of time, and therefore application of the standard boundary conditions requires the regeneration of the computational grid at every time step.

Moreover, realistic three-dimensional wings typically have control surfaces only over part of the wing span. Thus, a deflection of the control surface changes the section geometry only over a limited part of the span, resulting in discontinuities in the leading edge and/or the trailing edge of the wing at the inboard and outboard edges of the control surface. As a result, the use of body-fitted grids and the standard boundary conditions for these configurations will require special treatment of the discontinuities. This further enhances the complexity level of the analysis and consequently increases the computational effort necessary to solve the flow problem.

To keep the analysis simple and relatively inexpensive, the two issues mentioned above have been circumvented by introducing alternate linearized boundary conditions to model the effect of the control surface. This is done by using a body-fitted grid for the wing without any control surface deflection and including the effect of the control surface(s) through modified boundary conditions as explained below.

For the case of a control surface with deflection δ (positive for trailing edge down), the standard boundary condition is replaced by a linearized downward body velocity (plunge) of $U_\infty \delta$ for the region of the control surface.

For nonsteady control surface deflection with angular velocity $\dot{\delta}(t)$, the effect of control surface motion is linearized to yield an additional downward velocity of $(x - x_{\text{hinge}})\dot{\delta}(t)$.

Received March 6, 1990; revision received Dec. 27, 1990; accepted for publication Jan. 9, 1991.

*Senior Principal Engineer Scientist, Dept. 1XR, MC 18-86, 3855 Lakewood Blvd. Associate Fellow AIAA.

Combining the contributions of the deflection and motion of the control surface yields a total equivalent downward velocity of

$$V_{\text{body}}^{\text{equivalent}} = U_\infty \delta(t) + (x - x_{\text{hinge}}) \dot{\delta}(t)$$

Viscous Effects

The viscous region is assumed to be in instantaneous equilibrium with the outside potential flow. For the purpose of estimating viscous corrections, each computational span station is treated as being locally two dimensional, and the boundary layer computed using Cebeci's inverse technique.[14,15] An equivalent blowing velocity is obtained and used as a correction to the normal boundary condition to account for the addition or subtraction of mass flux through the surface to simulate the growth or decay of the displacement thickness on the wing surface. Any viscous effects on the wake are not accounted for in the present formulation.

For steady flows, the boundary layer is updated interactively with the potential flow solution, typically once for every 10 time steps of the inviscid flow analysis. As the time marching progresses, the combination of the potential flow and the boundary layer converges to a final steady flow solution.

For sinusoidal motion of the control surface, the effect of viscosity is studied using three different levels of approximation. The most elementary option uses the "frozen boundary layer" approach in which the unsteady analysis is performed using a time-invariant boundary layer computed for the converged steady flow problem at the mean control surface deflection. This option is computationally most efficient; however, it completely ignores any changes to the viscous effects due to the oscillation of the control surface.

The next higher level of complexity uses the "interpolated boundary layer." In this approach, converged steady flow boundary layers are computed at control surface deflections corresponding to the mean position and the two extreme positions of the sinusoidally oscillating control surface. During the analysis of the unsteady problem, the viscous corrections are estimated by linear interpolation of the stored data. This quasisteady analysis technique accounts for changes in the viscous effects due to geometry variations but ignores any phase effects caused by the unsteady potential flow.

The highest level of viscous corrections uses a "dynamic boundary layer" where the viscous effects are continually updated by revising the boundary layer at every time step used to compute the inviscid solution. This approach accounts for the correct viscous effects due to geometry changes and includes the influence of the time-dependent pressure variations from the potential flow analysis.

All three techniques discussed above have been investigated in this study.

Numerical Implementation

The formulation described above has been incorporated into a computer code TUFPAL (Transonic Unsteady Full Potential Aeroelastic Loads program). Some issues pertaining to the analysis of control surface loads are briefly discussed next.

Grid Generation

A sheared parabolic C-H grid system is used. The grid is clustered near the leading edge or the trailing edge, depending on the chordwise location of the control surface being modeled. The span stations are chosen such that the inboard and outboard side edges of the control surface are located in between successive computational stations. No special requirements are imposed on the grid near the hinge line.

Analysis Procedure

Typically, the unsteady analysis is done in two stages. During the first stage, a converged steady flow solution is obtained for the given freestream Mach number and incidence, at the mean position of the control surface. The time step used for this computation is chosen to optimize convergence to the steady flow solution. In the second stage, the unsteady solution is obtained starting from the converged steady flow solution. For this analysis, the time step is based on physical considerations such as number of time steps per cycle of oscillation. The total number of time steps needed for the analysis is determined by monitoring the response of the unsteady aerodynamic loads in time; the normal procedure is to continue the solution until the aerodynamic loads become periodic in time. It has been found from experience that typically two complete cycles of sinusoidal control surface motion are adequate for the solution to reach a steady-state periodic condition.

The unsteady results presented in this paper are limited to sinusoidal oscillation of the control surfaces. Unsteady pressure data is presented in the form of magnitude and phase distributions to compare with the available experimental data. These numerical values are estimated by postprocessing the time domain pressure data computed during the unsteady analysis.

Results and Discussion

Numerical results are presented here for a modern high aspect ratio transport wing (HARW). This wing has been tested by NASA, and experimental data is reported in Refs. 16 and 17. It is a computationally challenging problem because of the thick supercritical wing sections and associated effects of viscosity and separation. The wing has an aspect ratio of 10.76 and a leading-edge sweep of 28.8 deg, with the wing thickness ratio varying between 16% (at the root) and 12% (at the tip). Figure 1 shows a sketch of the wing plan form along with the location of the control surfaces. Computations were carried out to investigate the characteristics of the outboard aileron (control surface no. 9) and the leading-edge control surface (no. 4) that are located between span stations $\eta = 0.589$ and 0.794. The aileron covers 20% of the chord near the trailing edge, while the leading-edge device extends over 15% of the wing section.

Many of the numerical studies were done using a computational grid with 91 chordwise points (along the C line), 18 spanwise stations, and 15 points normal to the wing surface. Fifty-one of the 91 chordwise points were on the wing itself, and the remainder were on the wake. Some results were also obtained with additional grid points.

First, some results are presented for steady control surface deflections. Figure 2 shows the effect of deflecting the outboard aileron on the lifting pressure ($\Delta C_p = C_p^{\text{lower}} - C_p^{\text{upper}}$) when the freestream Mach number is 0.601 and $\alpha = 0.014$ deg. For all the cases analyzed, inviscid theory predicts higher values of overall loading on the wing as compared with the experiments. When the effect of viscosity is included, the agreement between theory and experiment improves consid-

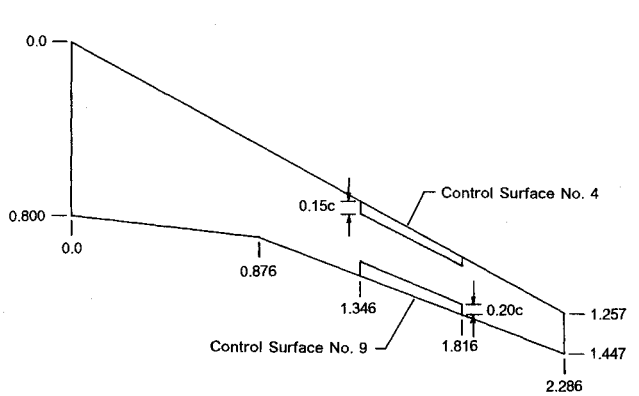

Fig. 1 Sketch of the high aspect ratio wing showing the control surfaces (all dimensions in meters).

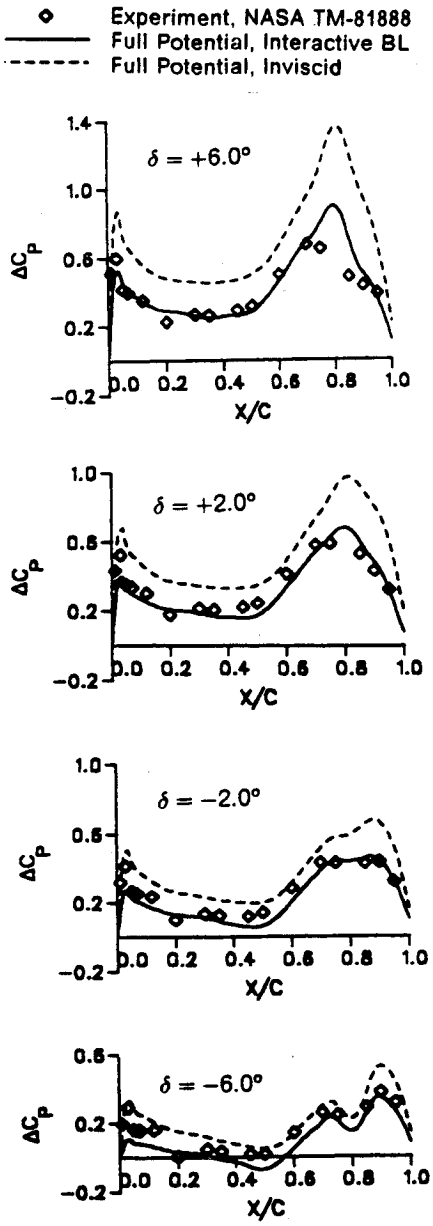

Fig. 2 Correlation between analysis and experiment for different static aileron deflections (M_∞ = 0.601, α = 0.014 deg). Aileron hinge is at 80% chord.

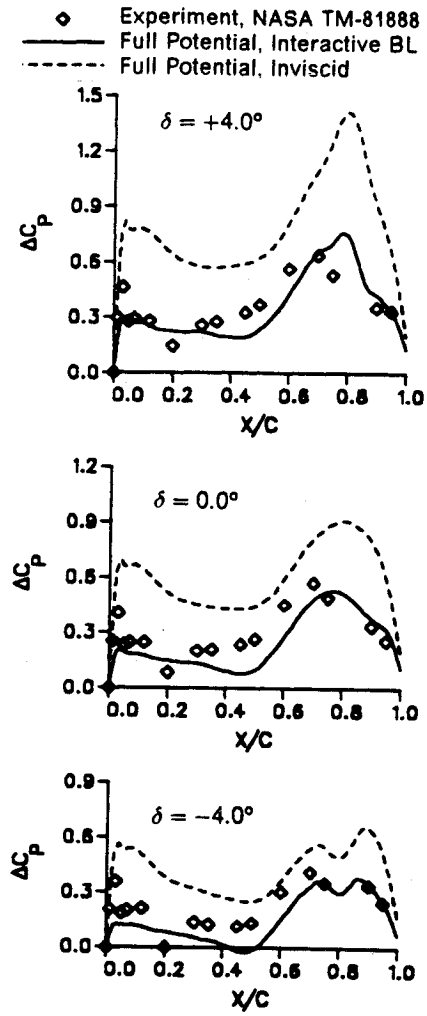

Fig. 3 Correlation between analysis and experiment for different static aileron deflections (M_∞ = 0.78, α = 0.013 deg).

erably. The computed values match experimental data quite well for negative and low positive aileron deflections. As the aileron deflection is increased, the computed values deviate from the experimental data over the aileron. This discrepancy is believed to be due to thickening of the boundary layer and development of a strong separation region.

Figure 3 shows the effect of static aileron deflection on the lifting pressure distributions for a freestream Mach number of 0.78 (α = 0.013 deg) when the flow becomes transonic. In this case also, the inviscid analysis overpredicts the lifting pressures. The results improve significantly when viscosity is included in the analysis; however, the agreement between the computed results and experimental data is not as good as in the previous case when the flow was fully subsonic.

The effect of deflecting the leading-edge control surface is shown in Fig. 4 for a freestream Mach number of 0.602 (α = 0.013 deg). The inviscid analysis predicts an overall loading higher than that from experiment. However, when the viscous corrections are included, the agreement with experiment is very good. No computations were made at the higher Mach number for the leading-edge control surface.

Figures 2–4 clearly demonstrate that the technique of representing control surface deflections by the equivalent body motion is satisfactory for modeling control surfaces with small deflections. They also indicate that modeling effects of viscosity in the computational model is very important for accurate prediction of steady aerodynamic loads due to control surfaces on thick supercritical wings. The control surface hinge moment is an important parameter of interest in practical applications. It is clear that the hinge moment predicted by the analysis would be significantly altered by including viscous effects in the analysis.

Another point of interest is the effect of static control surface deflection on the chordwise wing load distribution. When a control surface is deflected, it induces a change in the pressure at other chordwise locations of the wing section; however, the effect on the sectional lift and pitching moment are very different for the trailing-edge and leading-edge control devices. A positive deflection of the aileron not only increases the lifting pressure over the control surface itself but also increases the load, more or less uniformly, over the remainder of the wing section forward of the hinge (see Fig. 5). This results in a significant increase in the sectional lift accompanied by a nose-down pitching moment.

When the leading-edge control surface is given a positive deflection, the changes in the pressure distribution are largely confined to the region of the control surface itself and the immediate vicinity of the hinge on the fixed part of the wing section (see Fig. 5). This primarily results in a nose-up pitching moment with a very small influence on the sectional lift coefficient.

Next, results are presented for oscillating control surfaces. As mentioned earlier, the full potential analysis was performed in the inviscid mode as well as with three different levels of viscous correction; namely, 1) with a frozen boundary layer, 2) with an interpolated boundary layer, and 3) with a dynamic boundary layer.

The case of the aileron oscillating at 5 Hz (reduced frequency of 0.136 based on the root chord) with an amplitude of 4.02 deg (mean deflection of 0.01 deg) at a freestream Mach number of 0.601, and $\alpha = 0$ deg was studied first. Figure 6 presents the magnitude and phase of the lifting pressures ($\Delta C_p = C_p^{\text{lower}} - C_p^{\text{upper}}$) at the midspan location of the aileron, obtained from the present analysis using 200 time steps per cycle of aileron oscillation. Results from linear theory (obtained using the method of Ref. 18) are also shown, along with experimental data. For this case with a subcritical freestream flow, it was found that there is virtually no difference between the inviscid analysis and that with a frozen boundary layer. The addition of a time invariant boundary layer effectively acts as a modification to the thickness and camber distributions and does not influence the unsteady response for subcritical flow. However, the present inviscid method overpredicts the magnitude of the lifting pressure by a significant margin. Also, the phase angles predicted are lower than those from experiment by 15–30 deg. The results from linear theory are in reasonable agreement with experimental data for locations forward of the hinge line but worse than the present inviscid results over the aileron itself.

Figure 7 shows the effect of the different types of viscous corrections on the magnitude of the lifting pressure for the oscillating aileron subject to the same conditions as in Fig. 6. When the interpolated boundary layer is used, the magnitude of the unsteady lifting pressure agrees better with experimental data. The results improve further when a dynamic boundary layer is used; the magnitude of the lifting pressure matches that from experiment along most of the wing chord with a very respectable match over the aileron itself. Including the viscous effects also improves the correlation of the phase angles (by about 8 deg).

When the grid is modified such that there are 71 chordwise points on the wing, the magnitudes of the lifting pressure

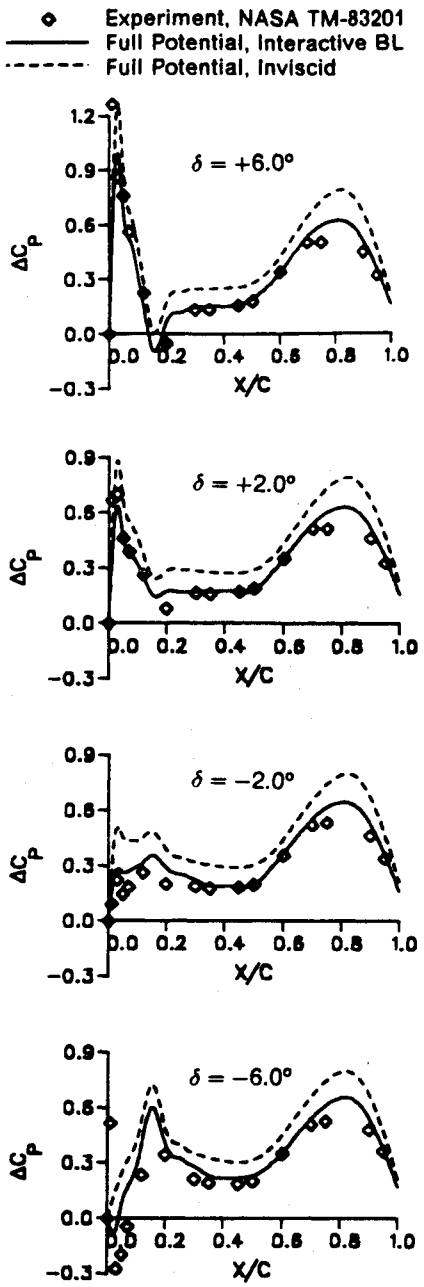

Fig. 4 Correlation between analysis and experiment for different static deflections of the leading-edge device ($M_\infty = 0.602$, $\alpha = 0.013$ deg). Hinge is located at 15% chord.

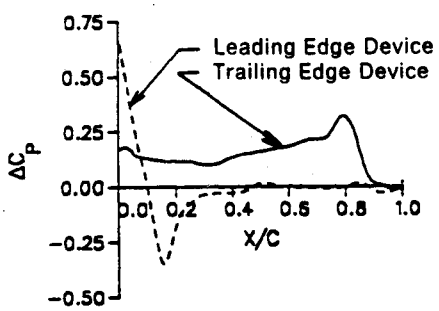

Fig. 5 Comparison of increments in the lifting pressure due to a +6 deg deflection for the aileron and the leading-edge device ($M_\infty = 0.60$, $\alpha = 0.01$ deg).

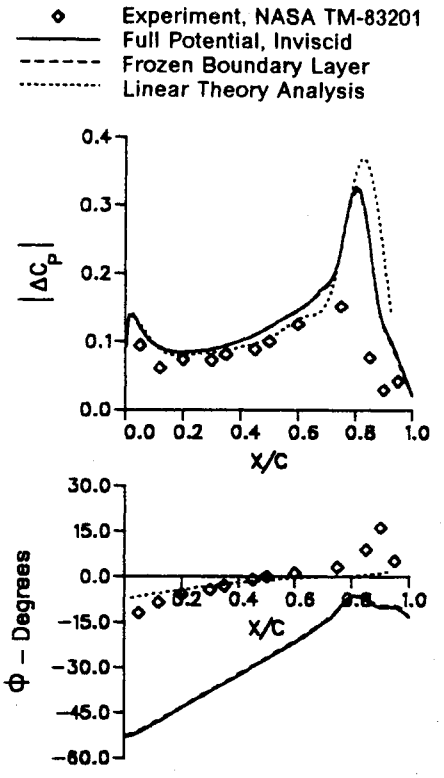

Fig. 6 Magnitude and phase of unsteady lifting pressure for oscillating aileron ($M_\infty = 0.601$, $\alpha = 0.0$ deg, $k = 0.136$, 200 time steps/cycle).

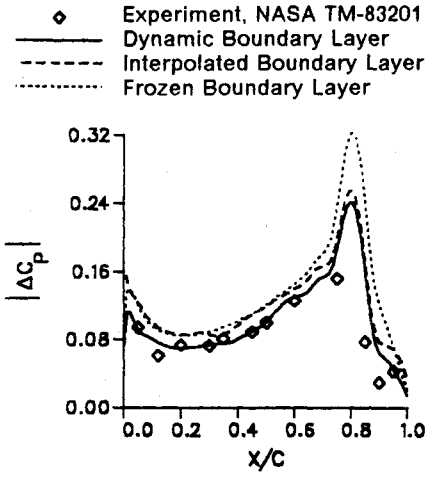

Fig. 7 Effect of viscous corrections on the magnitude of unsteady lifting pressure for oscillating aileron (M_∞ = 0.601, α = 0.0 deg, k = 0.136, 200 time steps/cycle).

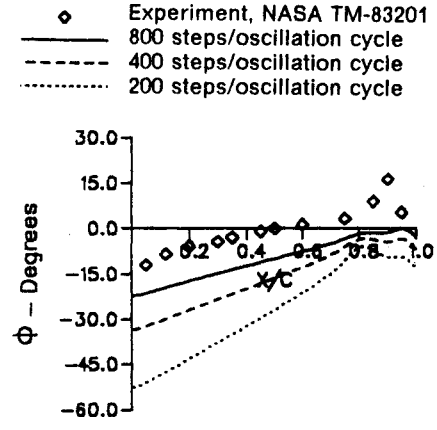

Fig. 8 Effect of computational time step on the phase response of the unsteady lifting pressure for oscillating aileron using frozen boundary-layer analysis (M_∞ = 0.601, α = 0.0 deg, k = 0.136).

improve further. However, the correlation of the phase angles deteriorates.

When the computational time step is decreased, the prediction of the phase angles improves considerably. This effect is shown in Fig. 8 for the aileron oscillating at 5 Hz in subcritical flow, for frozen boundary layer analysis. Using 800 steps per oscillation cycle gives the best correlation with experimental data. Similar results are obtained for analysis with a dynamic boundary layer. Interestingly, it is also found that using smaller time steps has an adverse effect on the lifting pressure magnitudes; they tend to increase slightly with decreasing time step size.

When the aileron is oscillated at higher frequencies (10 and 15 Hz) the advantage of using the full-potential analysis becomes more noticeable. At these higher frequencies, the prediction of phase angles from linear theory becomes increasingly inaccurate, whereas the full-potential method with viscous corrections maintains its accuracy.

Figure 9 shows results for the aileron oscillating at 15.01 Hz in a supercritical freestream (M_∞ = 0.782). Results from the present analysis are compared with experimental data and linear theory. For this case, when the flowfield includes regions of supersonic flow, the inviscid analysis and frozen boundary-layer approach yield slightly different results. The lifting pressure magnitudes from both of these methods correlate quite well with experimental data; the frozen boundary-layer approach being slightly more accurate. Phase angles obtained using 800 time steps per oscillation cycle (with a frozen boundary layer) are in very good agreement with experimental data. It may be noted that results from linear

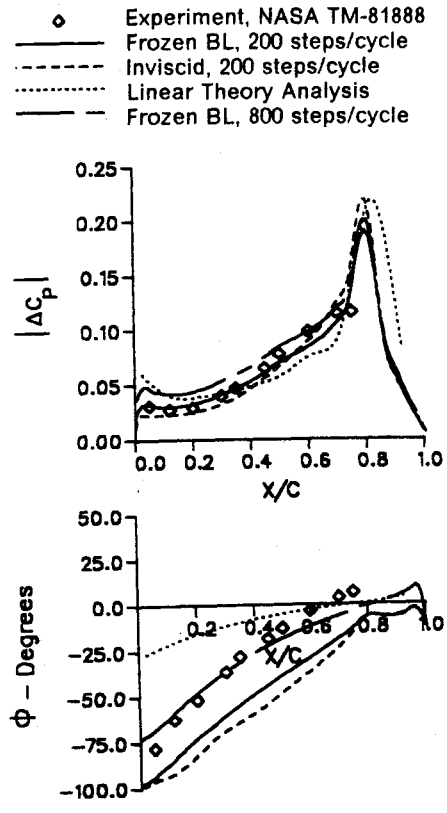

Fig. 9 Magnitude and phase of the unsteady lifting pressure for oscillating aileron (M_∞ = 0.782, α = 0.0 deg, k = 0.313).

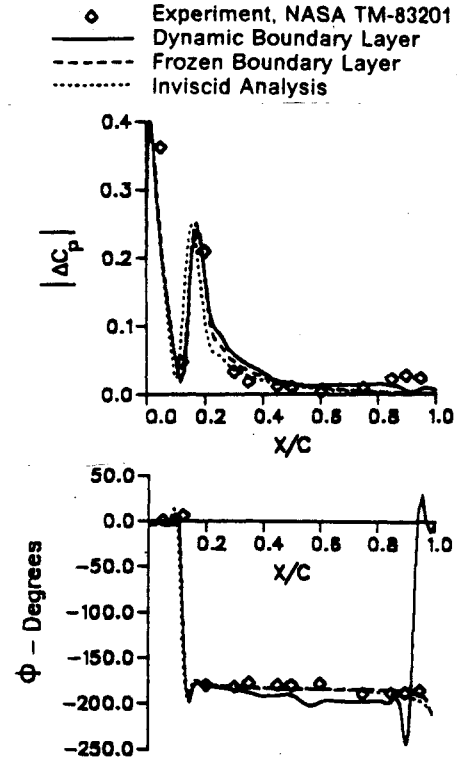

Fig. 10 Magnitude and phase of the unsteady lifting pressure for oscillating leading-edge device (M_∞ = 0.602, α = 0.0 deg, k = 0.136, 200 time steps/cycle).

theory are not very accurate for this case. In this case also, decreasing the time step size tends to have an adverse effect on the accuracy of the lifting pressure magnitude.

For this case, the results tend to get worse when the dynamic boundary layer is used. This surprising behavior is believed

to be due to the absence of wake effects and the strong interaction at the trailing edge in the present viscous model. Neglecting these effects tends to overpredict the boundary-layer displacement thickness, especially near the trailing edge. It is expected that using a better model for viscous corrections, including wake effects, will improve the results.

From the above data, it is clear that viscous effects play a significant part in the unsteady aerodynamics of trailing-edge control surfaces for wings with thick supercritical sections. The prediction of the magnitude of the unsteady response is considerably improved by including the correct viscous effects. However, accurate evaluation of the phase response depends primarily on the time step used for the inviscid analysis.

Figure 10 presents data for a leading-edge control surface oscillating at 5.01 Hz when the freestream Mach number is 0.602 and $\alpha = 0.0$ deg. As seen before for the case of the trailing-edge control surface, the results of inviscid full-potential analysis and the frozen boundary-layer analysis are almost identical. The magnitudes of the lifting pressure predicted by the full-potential analysis are in quite good agreement with experimental data over most of the chord length, except near the trailing edge. Using a dynamic boundary layer does not improve the results significantly. The phase angles are predicted quite accurately by the present analyses everywhere except near the trailing edge. The lifting pressures are either nearly in phase (over the control surface) or almost exactly out of phase. Additional results and computational times are given in Ref. 19.

Conclusions

A numerical method based on a time-accurate solution of the transonic full-potential equation for the prediction of steady and unsteady loads due to control surfaces on three-dimensional wings has been presented. The method uses an equivalent body velocity to model control surfaces and avoids the need for time-dependent grids and interpolation between computational span stations. Results are presented for a modern high aspect ratio transport wing and compared with experimental data, as well as with linear theory analysis. The major conclusions from this study are as follows.

1) Using the modified boundary condition to model control surfaces is valid both for steady and unsteady control surface deflections provided they are not too large.

2) Modeling of viscous effects is very important for accurately estimating the loads due to static control surface deflections. The effects of viscosity are more pronounced in transonic flows than in purely subsonic flows.

3) The effect of a steady deflection on the sectional lift and moment is very different for the trailing-edge and leading-edge control devices. The trailing-edge control surface produces a change in the pitching moment that accompanies the increment in the lift. On the other hand, the leading-edge device primarily causes a pitching moment change with minimal effect on the local lift.

4) Inviscid analysis is typically not adequate to predict the magnitude of unsteady loads due to oscillating trailing-edge control surfaces. Viscous corrections are needed. However, the viscous corrections do not improve the phase angle predictions significantly.

5) Increasing the number of chordwise grid points improves the prediction of the magnitudes of the lifting pressure at the expense of the phase correlation.

6) Accurate estimates of the phase response can be made by decreasing the time step used for the potential flow analysis, even with a frozen boundary layer. However, using smaller time steps tends to overpredict the magnitude of the unsteady response.

7) Accurate unsteady results can be computed efficiently by a moderate time step analysis with viscous corrections to obtain the lifting pressure magnitudes and a small time step frozen boundary-layer analysis for accurate phase angles.

8) For the leading-edge control surface, the inviscid analysis is already in quite good agreement with experiment, indicating a much smaller role played by viscosity.

Acknowledgment

This research was conducted under the independent research and development program of the McDonnell Douglas Corporation.

References

[1]Sotomayer, W. A., and Borland, C. J., "Numerical Computation of Unsteady Transonic Flow about Wings with Flaps," AIAA Paper 85-1712, July 1985.

[2]Isogai, K., and Suetsugu, K., "Numerical Calculation of Unsteady Transonic Potential Flow over Three-Dimensional Wings with Oscillating Control Surfaces," *AIAA Journal*, Vol. 22, No. 4, 1984, pp. 478–485.

[3]Chang, K. C., Alemdaroglu, N., Mehta, U., and Cebeci, T., "Further Comparisons of Interactive Boundary-Layer and Thin-Layer Navier-Stokes Procedures," AIAA Paper 87-0430, Jan. 1987.

[4]Melnik, R. E., and Brook, W., "The Computation of Viscid-Inviscid Interaction on Airfoils with Separated Flow," *Numerical and Physical Aspects of Aerodynamic Flows III*, Springer-Verlag, New York, 1986, pp. 77–101.

[5]Cebeci, T., Chen, L. T., and Chang, K. C., "An Interactive Scheme for Three-Dimensional Transonic Flows," *Numerical and Physical Aspects of Aerodynamic Flows III*, Springer-Verlag, New York, 1986, pp. 412–431.

[6]Woodson, S. H., DeJarnette, F. R., and Campbell, J. F., "An Interactive Three-Dimensional Boundary-Layer Method for Transonic Flow Over Swept Wings," AIAA Paper 89-0112, Jan. 1989.

[7]Malone, J. B., and Sankar, N. L., "Numerical Solutions of 2-D Unsteady Transonic Flows Using Coupled Potential-Flow/Boundary-Layer Methods," AIAA Paper 84-0268, Jan. 1984.

[8]Le Balleur, J. C., and Girodroux-Lavigne, P., "A Viscous-Inviscid Interaction Method for Computing Unsteady Transonic Separation," *Numerical and Physical Aspects of Aerodynamic Flows III*, Springer-Verlag, New York, 1986, pp. 252–271.

[9]Howlett, J. T., "Viscous Flow Calculations for the AGARD Standard Configuration Airfoils with Experimental Comparisons," *Transonic Unsteady Aerodynamics and Aeroelasticity 1987*, NASA-CP-3022, Pt. 2, 1987, pp. 313–330.

[10]Rizzetta, D. P., and Borland, C. J., "Numerical Solution of Three-Dimensional Unsteady Transonic Flow Over Wings Including Inviscid/Viscous Interactions," AIAA Paper 82-0352, Jan. 1982.

[11]Stone, H. L., "Iterative Solution of Implicit Approximations of Multi-Dimensional Partial Differential Equations," *SIAM Journal of Numerical Analysis*, Vol. 5, No. 3, 1968, pp. 530–558.

[12]Malone, J. B., and Sankar, N. L., "Application of a Three-Dimensional Steady and Unsteady Full Potential Method for Transonic Flow Computations," AFWAL-TR-84-3011, Flight Dynamics Lab., Air Force Wright Aeronautical Labs., Wright-Patterson AFB, OH, 1984.

[13]Malone, J. B., and Sankar, N. L., "Full Potential Solutions for Transonic Flows about Airfoils with Oscillating Flaps," AIAA Paper 84-0298, Jan. 1984.

[14]Cebeci, T., and Schimke, S. M., "The Calculation of Separation Bubbles in Interactive Turbulent Boundary Layers," *Journal of Fluid Mechanics*, Vol. 131, June 1983, pp. 305–317.

[15]Cebeci, T., Clark, R. W., Chang, K. C., Halsey, N. D., and Lee, K., "Airfoils with Separation and the Resulting Wakes," *Journal of Fluid Mechanics*, Vol. 163, Feb. 1986, pp. 323–347.

[16]Sandford, M. C., Ricketts, R. H., and Cazier, F. W., Jr., "Transonic Steady- and Unsteady-pressure Measurements on a High Aspect Ratio Supercritical Wing Model with Oscillating Control Surfaces," NASA-TM-81888, Dec. 1980.

[17]Sandford, M. C., Ricketts, R. H., and Watson, J. J., "Subsonic and Transonic Pressure Measurements on a High Aspect Ratio Supercritical Wing Model with Oscillating Control Surfaces," NASA-TM-83201, Nov. 1981.

[18]Giesing, J. P., Kalman, T. P., and Rodden, W., "Subsonic Unsteady Aerodynamics for General Configurations, Parts I and II," AFFDL-TR-71-5, Flight Dynamics Lab., Air Force Wright Aeronautical Labs, Wright-Patterson AFB, OH, 1971.

[19]Bharadvaj, B. K., "Computation of Steady and Unsteady Control Surface Loads in Transonic Flow," AIAA Paper 90-0935, April 1990.